Fibroblast Activation Protein Inhibitor Imaging in Nonmalignant Diseases: A New Perspective for Molecular Imaging

Christian Schmidkonz[1,2], Torsten Kuwert[1], Armin Atzinger[1], Michael Cordes[1], Georg Schett[3], Andreas Ramming[3], and Theresa Götz[2]

[1]*Department of Nuclear Medicine, Friedrich–Alexander University Erlangen–Nürnberg and University Hospital Erlangen, Erlangen, Germany;* [2]*Institute for Medical Engineering, Technical University of Applied Sciences Amberg–Weiden, Weiden, Germany; and* [3]*Rheumatology and Immunology, Department of Internal Medicine 3, Friedrich–Alexander University Erlangen–Nürnberg and University Hospital Erlangen, Erlangen, Germany*

Fibroblast activation protein-α (FAP-α) is a type II transmembrane glycoprotein that is overexpressed in activated fibroblasts such as those in the stroma of tumors or in the fibrotic processes accompanying various benign diseases. The recent development and clinical implementation of radiolabeled quinolone-based tracers suitable for PET that act as FAP inhibitors (FAPIs) have opened a new perspective in molecular imaging. Although multiple studies have investigated the use of FAPI imaging in cancer, evidence concerning its use in nonmalignant diseases is still scarce. Herein, we provide a comprehensive review of FAPI imaging in nonmalignant diseases to clarify the current and potential role of this class of molecules in nuclear medicine.

Key Words: fibroblast activation protein; inflammatory diseases; PET; molecular imaging; fibrosis

J Nucl Med 2022; 63:1786–1792
DOI: 10.2967/jnumed.122.264205

Fibroblast activation protein-α (FAP-α) is a type II transmembrane glycoprotein that is overexpressed in cancer-associated fibroblasts. These cells play a crucial role in the development of the tumor microenvironment, which is involved in tumor growth, migration, and progression (*1,2*). FAP-α is present on the cell membrane of activated fibroblasts in approximately 90% of epithelial neoplasms, whereas resting fibroblasts and most other cell types have little to no FAP expression. Therefore, the development of radiolabeled quinolone-based tracers suitable for PET that act as FAP inhibitors (FAPIs) was a major breakthrough in nuclear medicine (*3–7*). Direct comparisons between FAPIs and the dominant PET tracer in oncology in the last 40 years, ^{18}F-FDG, raise hopes for more sensitive and specific molecular imaging techniques that might also guide the way for novel theranostic treatment options (*8,9*).

However, fibroblast activation is not confined only to tumors but also occurs in immune-mediated diseases. Indeed, inflammation is directly linked to mesenchymal stromal activation, which leads to tissue damage. Activated FAP-positive fibroblasts play a major role in this process and can acquire heterogeneous activation states. Catabolic FAP-positive extracellular matrix–degrading phenotypes of fibroblasts are associated with, for example, cartilage destruction and bone erosions, as seen in rheumatoid arthritis (*10*). On the other hand, mesenchymal stromal activation can also result in their differentiation into FAP-positive extracellular matrix–producing fibroblasts positive for purine-rich box1, which is the dominant phenotype in fibrotic diseases. Fibrotic diseases such as systemic sclerosis (SSc) and IgG4-related disease (IgG4-RD) are characterized by fibroblast activation and an excessive accumulation of extracellular matrix, which disrupts the physiologic tissue architecture and often leads to severe dysfunction of the affected organs. Fibrotic tissue responses across different diseases have been estimated to account for up to 45% of deaths in high-income countries and cause a socioeconomic burden of tens of billions of U.S. dollars per year (*11*). Because of the elevated clinical and economic relevance of these disease groups, a noninvasive imaging approach toward accurately detecting and quantifying mesenchymal tissue responses would be desirable (*6*). However, assessment of the molecular dynamics of mesenchymal stromal activation and fibrosis remains challenging (*12*). In this review, we provide an overview of the use of FAPI PET/CT in nonmalignant diseases.

FAPI IMAGING IN IgG4-RD

Despite being inflammatory, immune-mediated diseases are associated with substantial activation of tissue-resident fibroblasts, resulting in fibrosis and organ damage. IgG4-RD is a paradigm of the inflammation-versus-fibrosis dichotomy: it is characterized by both autoimmune inflammation and tumefactive tissue fibrosis, with a predilection for the pancreas, salivary glands, kidney, aorta, and other organs (*13*). Although antiinflammatory drugs can reduce inflammatory activity in IgG4-RD, they have only a limited effect on the fibrotic disease component (*14*). During the disease course, there is a progression from a proliferative phenotype that is characterized by dense inflammatory lymphoplasmocytic infiltrates to a fibrotic phenotype with sparse cellular infiltrates but a greater degree of fibrosis (*15*).

In a cross-sectional clinical study, 27 patients with histologically confirmed IgG4-RD underwent both ^{18}F-FDG PET/CT and ^{68}Ga-FAPI-04 PET/CT, as well as MRI and histopathologic assessment (*12*). In a longitudinal approach, ^{18}F-FDG PET/CT and ^{68}Ga-FAPI-04 PET/CT data were evaluated before and after immunosuppressive treatment and were correlated with MRI and clinical data. Dual-tracer imaging revealed 3 distinct phenotypes of disease: proliferative, mixed,

Received Aug. 12, 2022; revision accepted Sep. 13, 2022.
For correspondence or reprints, contact Christian Schmidkonz (christian.schmidkonz@uk-erlangen.de).
Published online Sep. 15, 2022.

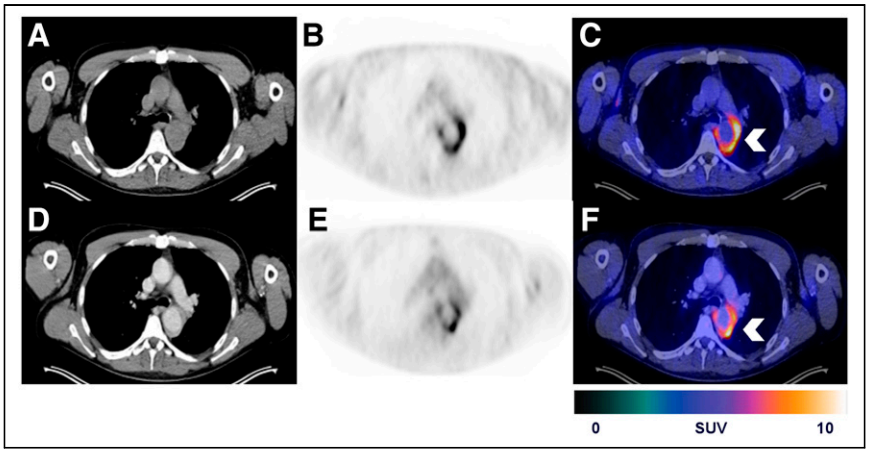

FIGURE 1. ^{68}Ga-FAPI-04 PET/CT (A–C) and ^{18}F-FDG PET/CT (D–F) images of man with histologically confirmed IgG4-RD. Tissue mass surrounding thoracic aorta exhibits increased ^{68}Ga-FAPI-04 and increased ^{18}F-FDG accumulation (arrowheads), typical of mixed phenotype.

and fibrotic (Fig. 1). The proliferative phenotype was characterized by intense lymphocyte infiltration, whereas fibroblasts were abundant in the fibrotic phenotype. Although the ^{18}F-FDG signal was positive in the inflammatory and mixed phenotypes, the fibrotic phenotype remained negative on ^{18}F-FDG PET/CT but positive on ^{68}Ga-FAPI-04 PET/CT (Fig. 2). Follow-up imaging revealed that antiinflammatory treatment of IgG4 manifestations significantly reduced ^{18}F-FDG PET uptake in more than 90% of inflammatory lesions. In contrast, fibrotic lesions demonstrated only a partial reduction in uptake after antiinflammatory treatment. Furthermore, more than 50% of active ^{68}Ga-FAPI-04 lesions were persistently detectable after 6 mo of antiinflammatory treatment. Interestingly, persistent fibrotic activity resulted in constant or further progression of the fibrotic lesion mass whereas lesions with a significant reduction in ^{68}Ga-FAPI-04 uptake decreased in size. These findings suggest that ^{18}F-FDG–negative IgG4-RD manifestations should not be misinterpreted as functionally inactive and that patients with ^{68}Ga-FAPI-04–positive lesions may require different forms of treatment because therapies that focus on proliferative disease features such as glucocorticoids may be sufficient to stop fibrosis.

Because of the development of specific treatments tackling fibrotic responses, such as pirfenidone or inhibitors of the transcription factor purine-rich box1, ^{68}Ga-FAPI-04 PET/CT might be an ideal tool to detect shifts from inflammatory to fibrotic disease and for evaluation of the treatment response in IgG4-RD (*16*). Luo et al. evaluated the use of ^{18}F-FDG PET/CT and ^{68}Ga-FAPI-04 PET/CT in 26 patients in a prospective cohort study (*17*). They compared the rates of PET/CT positivity for the involved organs and the respective uptake values of IgG4-RD lesions. Although ^{68}Ga-FAPI-04 PET/CT was visually positive for detecting involvement of IgG4-RD in all patients, ^{18}F-FDG PET/CT results were positive in 24 patients (92%). In the 136 involved organs, ^{68}Ga-FAPI-04 PET/CT additionally detected 18 involved organs (13%) in 13 patients (50%), compared with ^{18}F-FDG PET/CT. All ^{18}F-FDG–avid lymph node involvement was missed by ^{68}Ga-FAPI-04 PET/CT. This is most likely explained by the missing storiform fibrosis pattern typical of IgG4-RD. Visual comparison of the uptake and extension of the involved organs revealed higher uptake and a more pronounced disease extension in the pancreas, bile duct/liver, and salivary glands for ^{68}Ga-FAPI-04 PET/CT than for ^{18}F-FDG PET/CT. A similar pattern was observed for the quantitative comparison of SUV_{max}, which demonstrated significantly higher values for ^{68}Ga-FAPI-04 PET/CT than for ^{18}F-FDG PET/CT. The authors concluded that ^{68}Ga-FAPI-04 PET/CT might be a promising tool for the assessment of IgG4-RD.

NOTEWORTHY

- FAPI imaging has a potential role in nonmalignant diseases.
- FAPI PET/CT is the only available imaging modality that can directly assess the dynamics of PF.
- FAPI PET/CT can differentiate inflammatory from fibrotic disease.
- An early FAPI signal in acute myocardial infarction is a predictor of adverse left ventricular remodeling.

FAPI IMAGING IN PULMONARY FIBROSIS (PF)

PF, as an example of mesenchymal stroma activation, can arise as an idiopathic disorder or in the context of autoimmune diseases such as SSc. SSc is a prototypical fibrotic disease that shows PF development in 84% of patients and is their leading cause of death (*18,19*). Currently, the progression of PF in SSc is judged by measuring the accrual of lung damage represented by fibrosis on CT and the functional decline in forced vital capacity. This approach requires long-term follow-up to detect changes and does not directly assess the activity of tissue remodeling at the time of assessment. Furthermore, it often does not predict the course of PF in individual patients and does not enable appropriate risk stratification. In a single-center pilot study, Bergmann et al. tested the hypothesis that quantification of fibroblast activation by ^{68}Ga-FAPI-04 PET/CT can be correlated with PF activity and disease progression in patients with SSc (*20*). The authors recruited 21 patients who had SSc-associated PF confirmed by high-resolution CT (HRCT) and who fulfilled the classification criteria of the American College of Rheumatology and the European League Against Rheumatism. Another 21 patients without SSc or PF, who were examined for other clinical reasons, were enrolled as controls. All patients underwent ^{68}Ga-FAPI-04 PET/CT and standard-of-care procedures, including HRCT and pulmonary function tests at baseline. The patients were followed for 6 mo with HRCT and pulmonary function tests for a comparison with the baseline ^{68}Ga-FAPI-04 PET/CT results and for prediction of PF progression. A subset of patients treated with the antifibrotic drug nintedanib underwent follow-up at between 6 and 10 mo, with use of ^{68}Ga-FAPI-04 PET/CT to determine the changes in PF over time. The authors found that ^{68}Ga-FAPI-04 accumulated in fibrotic areas of the lungs in patients with SSc-associated PF, whereas there was no significant uptake in the control group (Fig. 3). ^{68}Ga-FAPI-04 uptake was significantly higher in patients with extensive disease, with previous progression of PF, or with higher clinical activity scores than those with limited disease, previously stable interstitial lung disease, or low clinical activity scores. Increased ^{68}Ga-FAPI-04 uptake at baseline was associated with progression of PF independently of the

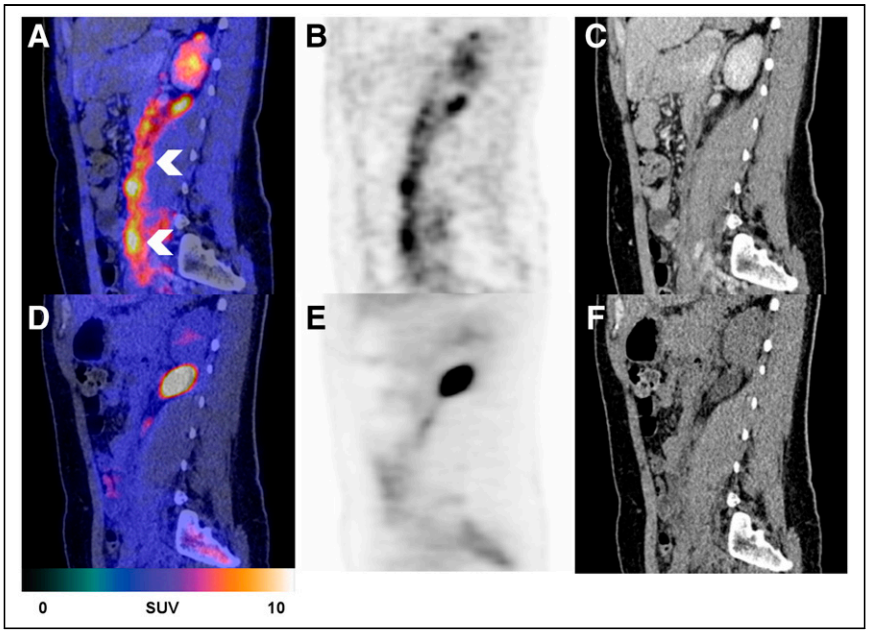

FIGURE 2. ^{68}Ga-FAPI-04 PET/CT (A–C) and ^{18}F-FDG PET/CT (D–F) images of woman with histologically confirmed IgG4-RD presenting with ^{68}Ga-FAPI-04–positive retroperitoneal mass (arrowheads) that demonstrates no significant ^{18}F-FDG uptake, typical of fibrotic phenotype.

extent of the involvement on HRCT and the forced vital capacity at baseline. Furthermore, the authors provided initial evidence that changes in ^{68}Ga-FAPI-04 scores over time might correlate with changes after treatment with nintedanib, the first approved fibroblast-targeting antifibrotic drug. They concluded that, in contrast to other techniques such as pulmonary function tests, which measure the cumulative result of tissue damage, ^{68}Ga-FAPI-04 PET/CT is the only available imaging modality that can directly assess the dynamics of PF. Further studies are warranted to clarify whether ^{68}Ga-FAPI-04 PET/CT might improve the risk assessment of patients with SSc-associated PF and allow earlier, more accurate treatment and dynamic monitoring of the molecular response to fibroblast-targeting therapies.

Röhrich et al. evaluated the static and dynamic imaging properties of ^{68}Ga-FAPI-46 PET/CT in 15 patients with fibrotic interstitial lung disease (fILD) and suspected lung cancer (*21*). Static PET/CT scans and dynamic scans were performed on 12 patients and an additional 3 patients, respectively. SUV measurements of 55 morphologically typical fibrotic lesions on CT and 3 lung cancer lesions yielded a considerably elevated uptake at each of the static imaging time points. The SUV_{max} and SUV_{mean} of fILD and the lung cancer lesions decreased over time, with a more pronounced decrease in fILD than in lung cancer lesions. Because of the decreasing background activity over time, the fILD manifestations demonstrated relatively stable target-to-background ratios, whereas the target-to-background ratios of the lung cancer manifestations tended to increase during the sequential PET examinations. These findings highlight the potential use of quantitative PET imaging at sequential time points to differentiate between malignant and fibrotic lesions. Röhrich et al. also evaluated the use of dynamic PET acquisitions. Although fILD lesions showed an early peak in tracer accumulation with a slowly decreasing signal intensity over time, lung cancer manifestations presented an increasing time–activity curve with a delayed peak and gradual washout. In contrast to the current imaging standard (HRCT, which is not capable of determining disease activity), ^{18}F-FDG PET/CT is of limited use for the assessment of antifibrotic drugs (*22*). Röhrich et al. evaluated FAP expression using immunohistochemistry in both human fILD biopsies and whole-lung sections of Nedd4-22/2 mice, serving as a gold standard. FAP-positive areas were localized to the transition zone between healthy lung tissue and fibrotic areas in human fILD sections. In Nedd4-22/2 mice, healthy lung parenchyma demonstrated only low FAP expression, but fibrotic lesions exhibited FAP upregulation. These impressive results suggest a promising role for FAPI imaging in fibrotic lung diseases for evaluating disease activity and the response to antifibrotic treatment.

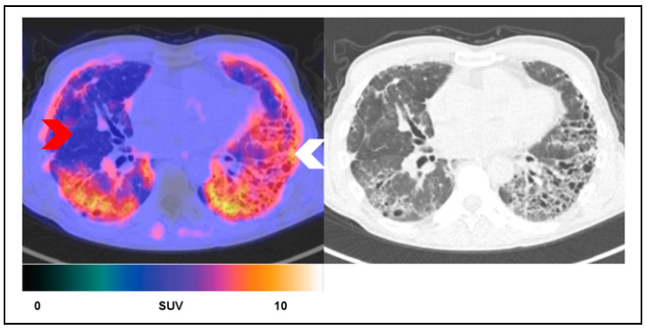

FIGURE 3. ^{68}Ga-FAPI-04 PET/CT images of man with SSc-associated PF. ^{68}Ga-FAPI-04 uptake is increased in fibrotic lung areas (white arrowhead), whereas there is no significant ^{68}Ga-FAPI-04 accumulation in healthy nonfibrotic lung tissue (red arrowhead).

FAPI IMAGING IN CARDIOVASCULAR DISEASES

In cardiac disease, myocardial fibrosis contributes to the development and progression of heart failure. Myocardial fibroblast activation is essential for repair and regeneration after myocardial damage, such as from myocardial infarction or progressive heart failure. Several studies have described the molecular pathways leading to the activation of quiescent fibroblasts, which have emerged as attractive targets to support cardiac repair and prevent loss of function (*23,24*). Heart failure related to the development of fibrosis is among the most common adverse effects of modern cancer therapy, which includes radiotherapy, conventional chemotherapy, immunotherapy, and targeted therapy (*25,26*). In a retrospective study, Siebermair et al. analyzed the datasets of 32 patients who underwent ^{68}Ga-FAPI-04 PET/CT for cancer staging (*27*). All examinations were analyzed visually and quantitatively with respect to cardiac uptake. Quantitative measurements were correlated with clinical covariates, including previous anticancer treatment, age, left ventricular ejection fraction (LVEF), coronary artery disease, and cardiovascular risk factors. Of the 32 patients, 6 (18.8%) demonstrated visually increased uptake clearly above the background level, and on quantitative analysis, this uptake was also significantly higher than in remote myocardium. No significant differences with respect to cancer entity and

applied chemotherapy and immunotherapy were observed. In contrast, a significant correlation of coronary artery disease, age, and LVEF with uptake could be demonstrated. The authors concluded that the measurement of myocardial fibroblast activation using ^{68}Ga-FAPI-04 PET/CT might be useful for risk stratification regarding the early detection or progression of coronary artery disease and left ventricular remodeling.

In a larger cohort of 229 patients, Heckmann et al. retrospectively analyzed the correlation between myocardial uptake, cardiovascular risk factors, and metabolic disease in patients with metastatic cancer (*28*). The modeling cohort comprised 185 patients—and the confirmatory cohort 44 patients—who were analyzed by application of the American Heart Association 17-segment model of the left ventricle. Multivariate regression models revealed a significant correlation among left ventricular uptake, hypothyroidism, a body mass index above 25 kg/m^2, previous radiation to the chest, previous intake of platinum derivates, and a history of diabetes mellitus. Interestingly, although a single cardiovascular risk factor led to a relatively mild increase in signal intensity, patients with multiple risk factors exhibited a more pronounced increase. FAPI uptake was most noticeable in patients with arterial hypertension and metabolic diseases, characterized by diabetes mellitus and obesity. These findings are also supported by animal data from diabetes mellitus models and transaortic constriction, which promote cardiac hypertrophy and excessive cardiac fibrosis (*29,30*). On the basis of their findings, Heckmann et al. concluded that high ^{68}Ga-FAPI signal intensities are linked to cardiovascular risk factors, specifically arterial hypertension, diabetes mellitus, and obesity. They suggest further studies to systematically compare ^{68}Ga-FAPI PET/CT scans with other cardiac imaging modalities and possibly gene expression profiles to pave the way to clinical practice.

In acute myocardial infarction, an immediate organized inflammatory immune reaction triggers the activation of fibroblasts (*31,32*). Activated myofibroblasts migrate to injured tissue and contribute to fibrotic scar formation, which preserves the wall architecture and prevents mechanical complications such as ventricular wall rupture. However, excessive fibrosis development is suggested to cause a progressive decline in ventricular systolic function, potentially leading to the development of chronic heart failure (*33*). Current imaging modalities such as MRI assess these structural changes primarily at a disease stage at which the damage has already occurred (*34*). Therefore, the assessment of local fibroblast activation suggesting structural remodeling after ischemia might be a promising approach to risk stratification. In a proof-of-concept study, Kessler et al. examined the pattern of ^{68}Ga-FAPI-46 uptake in the myocardium of patients after acute myocardial infarction to investigate its association with the affected coronary artery and to correlate the ^{68}Ga-FAPI-46 signal with biomarkers of myocardial damage, including parameters of left ventricular function (*35*). Ten patients who had undergone ^{68}Ga-FAPI-46 PET/CT after percutaneous coronary intervention for risk stratification after acute myocardial infarction were retrospectively analyzed. Uptake patterns in polar maps and axial images were assessed according to the 17-segment model of the American Heart Association. To assess the level of agreement between the localized uptake and the myocardial areas supplied by the culprit vessel, a visual grading scale was established. Furthermore, myocardial uptake was quantified and the myocardial volume of FAPI accumulation was determined and correlated with biomarkers of myocardial damage, including left ventricular function. On visual interpretation, PET/CT demonstrated moderate-to-intense myocardial uptake in all 10 patients. The affected myocardium showed a partial or complete match between uptake and the confirmed culprit lesion by coronary angiography in 44% and 56% of patients, respectively. Quantitative evaluation revealed a strong correlation between the myocardial volume of ^{68}Ga-FAPI-46 accumulation and the peak creatine kinase level but an inverse correlation between the myocardial volume of ^{68}Ga-FAPI-46 accumulation and left ventricular function. On the basis of these results, the authors concluded that the PET-derived volume of myocardial fibroblast activation can truly reflect the extent of myocardial injury after acute myocardial infarction. In contrast to the signal derived from cardiac MRI (CMR), which usually persists for months to years after local damage, predominantly reflecting fibrotic remodeling, ^{68}Ga-FAPI-46 PET/CT offers a functional modality to assess local damage with consecutive repair mechanisms within days of the ischemic event.

In a retrospective single-center study, Diekmann et al. tested the hypothesis that ^{68}Ga-FAPI-46 PET/CT reflects a myocardial signal early after acute myocardial infarction that is distinct from CMR-derived tissue characteristics and predicts later development of ventricular dysfunction (*36*). Their analysis included 35 patients who had undergone clinical resting myocardial perfusion SPECT, ^{68}Ga-FAPI-46 PET/CT, and CMR within 11 d after reperfusion therapy for acute myocardial infarction. Although the infarct size was determined from SPECT by comparison to a reference database, quantitative analysis of left ventricular tracer accumulation determined the extent of FAP upregulation. On the basis of late gadolinium enhancement derived from CMR, they found that the area of myocardial FAP upregulation was significantly larger than that of the SPECT perfusion defect or the infarct area. Interestingly, late gadolinium enhancement was detected in only 56% of FAP-positive segments, whereas an elevated T1 and T2 signal was visible in 74% and 68% of tracer-positive segments, respectively. Myocardial FAP volume correlated only weakly with simultaneously measured LVEF at baseline, whereas there was a significant inverse correlation with LVEF obtained at later follow-up. Altogether, the results of Diekmann et al. suggest that the area of elevated FAP signal extends beyond the injured infarct region and involves regions without prolonged T1 and T2 relaxation, which are CMR markers of interstitial fibrosis, infiltration, or edema. On the basis of their findings, the cell-based signal of fibroblast activation is distinct from CMR-derived interstitial characteristics and may be complementary. Early FAP signal was associated with a subsequent impairment of LVEF, suggesting that it might be a predictor of adverse left ventricular remodeling.

In a prospective study, Xie et al. explored the correlation of ^{18}F-NOTA-FAPI PET/CT with CMR parameters in patients with ST-segment elevation myocardial infarction who underwent successful primary percutaneous coronary intervention (*37*). They further investigated the value of ^{18}F-NOTA-FAPI imaging in predicting cardiac functional recovery, as well as the correlation of ^{18}F-NOTA-FAPI activity with circulating FAP and inflammatory biomarkers. They prospectively recruited 14 patients with first-time ST-segment elevation myocardial infarction after primary percutaneous coronary intervention and 14 sex-matched healthy controls who had completed ^{18}F-NOTA-FAPI PET/CT and blood sample collection. All patients underwent ^{18}F-NOTA-FAPI PET/CT and CMR, whereas 10 patients underwent additional follow-up CMR. Myocardial ^{18}F-NOTA-FAPI tracer accumulation was evaluated quantitatively for extent and intensity and correlated with myocardial injury biomarkers derived from CMR. Although no visible uptake was detected in healthy controls, localized but inhomogeneous myocardial ^{18}F-NOTA-FAPI uptake was observed in all patients with ST-segment elevation myocardial infarction; this uptake was greater than in the edematous and infarcted myocardium. Myocardial ^{18}F-NOTA-FAPI activity was

significantly associated with the myocardial biomarkers T2-weighted imaging, late gadolinium enhancement, and extracellular volume, at both per-patient and per-segment levels, but not with circulating FAP or inflammatory biomarkers. Furthermore, an inverse correlation was observed with the follow-up LVEF. To summarize these results, ^{18}F-NOTA-FAPI imaging is feasible for assessing myocardial damage and has prognostic value for cardiac recovery after myocardial infarction. Further larger studies are warranted to evaluate the potential role of ^{18}F-NOTA-FAPI PET/CT for the assessment of myocardial remodeling after myocardial infarction and to analyze fibroblast-targeted antifibrotic therapies.

Wu et al. retrospectively analyzed the use of ^{68}Ga-FAPI-04 PET/CT for the in vivo imaging of FAP expression in human arterial walls (*38*). Their study included 41 patients who underwent ^{68}Ga-FAPI-04 PET/CT either for suspected hepatic lesions or for IgG4-RD. Correlations were calculated of the uptake of ^{68}Ga-FAPI-04 in large arterial walls with the degree of calcification derived from CT and cardiovascular risk factors. Focal arterial ^{68}Ga-FAPI-04 uptake was detected in 1,177 arterial segments in all 41 patients. Analysis of all segments revealed a significant correlation between the extent of calcification and the intensity of uptake. Noncalcified arterial segments had significantly higher uptake than mildly calcified segments, whereas severely calcified segments exhibited the lowest uptake. Patients in the high-risk group, who had at least 4 cardiovascular risk factors, demonstrated significantly higher ^{68}Ga-FAPI-04 uptake than the low-risk group. Xie et al. concluded that ^{68}Ga-FAPI-04 PET/CT might have potential for imaging fibroblast activation in the arterial wall and thus might provide new insights into the pathologic mechanisms of arteriosclerosis.

Kupusovic et al. conducted a proof-of-concept study to assess ^{68}Ga-FAPI uptake in the pulmonary vein region of the left atrium after pulmonary vein isolation with cryoballoon ablation and radiofrequency ablation as a surrogate for thermal damage (*39*). Twelve patients who had undergone ^{68}Ga-FAPI PET after pulmonary vein isolation were included and compared with 5 patients without cardiac comorbidities who underwent ^{68}Ga-FAPI PET for tumor staging. In 10 of the 12 patients, significant ^{68}Ga-FAPI uptake was detected, whereas no uptake was observed in 2 patients or in any control patients. All postcryoballoon ablation patients had intense uptake, whereas in the radiofrequency ablation group, 2 patients had intense uptake, 1 patient had moderate uptake, and 2 patients had no uptake at all. Quantitative evaluation revealed significantly higher uptake in cryoballoon ablation patients than in radiofrequency ablation patients, suggesting that the cryoballoon ablation procedure causes a more pronounced fibroblast activation after tissue injury than does radiofrequency ablation. Future studies are warranted to assess whether this modality can contribute to a better understanding of the mechanisms of atrial fibrillation recurrence after pulmonary vein isolation.

Chen et al. explored the association of cardiac fibroblast activation with clinical and CMR parameters in patients with chronic thromboembolic pulmonary hypertension (CTEPH) (*40*). Thirteen CTEPH patients were prospectively enrolled and underwent ^{68}Ga-FAPI-04 PET/CT, right heart catheterization, and echocardiography; 11 of these patients additionally underwent CMR. Another 13 subjects without any cardiac morbidities comprised a control group to establish the reference range of cardiac ^{68}Ga-FAPI-04 uptake. Although there was no suspected cardiac ^{68}Ga-FAPI-04 uptake in the control group, 10 CTEPH patients (77%) showed increased inhomogeneous ^{68}Ga-FAPI-04 uptake in the right ventricle (RV), localized mainly in the free wall. Notably, increased ^{68}Ga-FAPI-04 uptake was also observed in the right atrium of 11 CTEPH patients but was significantly lower than in the RV. A significant correlation between the RV ^{68}Ga-FAPI-04 accumulation and the thickness of the RV wall was observed, whereas an inverse correlation was demonstrated with the RV fraction area change and the tricuspid annular plane systolic excursion (TAPSE) as indices of RV function. No significant correlation was found between PET and CMR parameters. On the basis of the correlation of both RV fraction area change and TAPSE with the increased ^{68}Ga-FAPI-04 accumulation, the authors suggested that FAP activation reflects longitudinal and transversal contraction of the overloaded RV in CTEPH. This might be of further importance because change in RV fraction area and TAPSE are related to survival in pulmonary hypertension (*41,42*). Thus, ^{68}Ga-FAPI-04 imaging may have the potential to be an effective means for assessing the outcome of CTEPH patients. The authors demonstrated that increased fibroblast activation reflects thickening of the RV wall and decreased RV contractile function. FAPI imaging might therefore be a promising approach toward assessing RV fibrosis in CTEPH patients and monitoring future tailored antifibrotic treatments.

Gu et al. prospectively enrolled 16 patients with pulmonary artery hypertension to investigate the feasibility of ^{68}Ga-FAPI-04 PET/CT for assessing RV fibrotic remodeling and the relationship of ^{68}Ga-FAPI-04 uptake with parameters of pulmonary hemodynamics and cardiac function (*43*). All patients underwent right heart catheterization and echocardiography for the assessment of pulmonary hemodynamics and cardiac function. Myocardial ^{68}Ga-FAPI-04 uptake was assessed visually and quantitatively as SUV_{max}. Of the 16 patients, 12 (75%) exhibited heterogeneous signal in the RV free wall and insertion point. Patients with a TAPSE of less than 17 mm, who were considered the impaired RV function group, had significantly higher uptake than those with a TAPSE of 17 mm or more in both the RV free wall and the insertion point, indicating that RV uptake of ^{68}Ga-FAPI-04 is associated with RV dysfunction. Furthermore, there was a significant positive correlation between cardiac ^{68}Ga-FAPI-04 uptake and total pulmonary resistance and the level of N-terminal pro–B-type natriuretic peptide. Gu et al. concluded that ^{68}Ga-FAPI-04 PET/CT is feasible for directly visualizing fibrotic remodeling of the RV in patients with pulmonary artery hypertension.

FAPI IMAGING IN BENIGN LESIONS ENCOUNTERED IN ONCOLOGIC IMAGING

Qin et al. retrospectively reviewed 129 PET/CT or ^{68}Ga-DOTA-FAPI-04 PET/MRI scans to identify foci of elevated uptake in the bones and joints (*44*). All lesions were categorized as malignant or benign disease. Elevated uptake of ^{68}Ga-DOTA-FAPI-04 in or around the bone or joint was found in 82 patients (63.6%). In total, 295 lesions were identified, including 94 malignant lesions (31.9%) and 201 benign lesions (68.1%). Although the malignant lesions were all classified as metastases, the benign lesions comprised osteofibrous dysplasia, degenerative bone disease, periodontitis, arthritis, and other inflammatory or trauma-related abnormalities. Quantitative analysis revealed significantly higher ^{68}Ga-DOTA-FAPI-04 uptake in bone metastases than in benign lesions, although there was some overlap between the 2 entities. Differences in SUV_{max} among subgroups of benign diseases were statistically significant, with much higher uptake in periodontitis. In a subgroup of 29 patients who underwent both

^{18}F-FDG and ^{68}Ga-DOTA-FAPI-04 PET, significantly more lesions with higher uptake were identified by ^{68}Ga-DOTA-FAPI-04 imaging. On the basis of these findings, the authors concluded that abnormal osseous ^{68}Ga-DOTA-FAPI-04 uptake should be carefully assessed in patients with malignant tumors to avoid misdiagnosis due to overlap of uptake between benign and malignant bone lesions. Furthermore, ^{68}Ga-DOTA-FAPI-04 PET also has the potential to locate and evaluate the extent of both malignant tumors and benign diseases in bones and joints.

Zheng et al. retrospectively reviewed 182 patients with various suspected cancers who underwent ^{68}Ga-FAPI-04 PET/CT to characterize benign lesions showing increased ^{68}Ga-FAPI-04 tracer accumulation (*45*). They detected 185 primary tumors and 360 benign lesions with uptake, including inflammatory processes, exostoses, hemorrhoids, fractures, and hepatic fibrosis. Lesions were diagnosed as benign on the basis of imaging findings, clinical information, or histologic biopsy. Quantitative analysis revealed a significantly higher SUV_{max} for malignant lesions than for benign lesions, but with a significant overlap between them. The authors concluded that some benign lesions can easily be diagnosed by a combination of CT findings, location, and clinical data but that some lesions still may be confused with malignant lesions or need further clarification.

FAPI IMAGING IN RHEUMATOID ARTHRITIS

In a preclinical evaluation and pilot clinical study, Ge et al. evaluated the novel tracer ^{18}F-AlF-NOTA-FAPI-04 for PET imaging of rheumatoid arthritis (*46*). In the inflamed joints of patients with rheumatoid arthritis, fibroblast-like synoviocytes are key effector cells that exacerbate the inflammatory destruction of adjacent articular cartilage and bone by producing matrix metalloproteinase enzymes and proinflammatory cytokines. FAP is highly expressed in rheumatoid arthritis–derived fibroblast-like synoviocytes and is a specific marker for disease activity. Ge et al. performed this pilot study to image activated fibroblast-like synoviocytes in vitro, in arthritic joints of mice with collagen-induced arthritis, and in 2 patients with rheumatoid arthritis. They found that the binding of ^{18}F-AlF-NOTA-FAPI-04 increased significantly in activated fibroblast-like synoviocytes compared with controls. Compared with ^{18}F-FDG imaging, ^{18}F-AlF-NOTA-FAPI-04 showed high uptake in inflamed joints in the early stage of arthritis, and this uptake correlated positively with arthritis scores. Furthermore, ^{18}F-AlF-NOTA-FAPI-04 PET/CT in 2 patients with rheumatoid arthritis revealed nonphysiologically high uptake in the synovium of arthritic joints. The authors concluded that ^{18}F-AlF-NOTA-FAPI-04 is a promising radiotracer for imaging of rheumatoid arthritis and might potentially complement current noninvasive diagnostic parameters.

FAPI IMAGING IN RENAL FIBROSIS

Kidney fibrosis leads to a progressive reduction in kidney function, ultimately resulting in kidney failure. To date, all diagnostic tools to detect kidney fibrosis have been invasive, requiring kidney biopsies with subsequent histologic validation. In a retrospective study, Conen et al. analyzed the PET data of 81 patients who received ^{68}Ga-FAPI-04, ^{68}Ga-FAPI-46, ^{68}Ga-PSMA, or ^{68}Ga-DOTATOC (*47*). Kidney function parameters were correlated with the SUV_{max} and SUV_{mean} of the renal parenchyma. The authors found a negative correlation between glomerular filtration rate and ^{68}Ga-FAPI uptake for both SUV_{max} and SUV_{mean}, which was not the case for ^{68}Ga-DOTATOC and ^{68}Ga-PSMA. Conen et al. concluded that this correlation suggests a specific binding of ^{68}Ga-FAPI rather than a potential unspecific retention in the renal parenchyma, underlining the potential value of ^{68}Ga-FAPI for the noninvasive quantitative evaluation of kidney fibrosis.

Zhou et al. evaluated the use of ^{68}Ga-FAPI-04 PET/CT in 13 patients with histologically confirmed renal fibrosis (*48*). All patients underwent renal puncture before undergoing ^{68}Ga-FAPI-04 PET/CT. The ^{68}Ga-FAPI-04 examinations found that 12 of the 13 patients had increased uptake. Furthermore, SUV_{max} and target-to-background ratios correlated with the pathology of kidney tissue. The authors concluded that ^{68}Ga-FAPI-04 PET/CT is a valuable tool to diagnose renal fibrosis without a biopsy.

CONCLUSION

The development of FAPIs suitable for PET/CT has opened a new chapter in molecular imaging. Besides their successful use in oncologic diseases, several studies presented in this review suggest a potential role for FAPI imaging in immune-mediated inflammatory and fibrotic diseases, as well as cardiovascular diseases, and for distinguishing between benign and malignant lesions. However, current data rely predominantly on retrospective analyses, and evidence is still scarce for many possible indications. Well-defined patient cohorts and, ideally, prospective randomized trials are needed to include FAPI imaging in guidelines and to fully exploit the potential of this novel imaging technique.

DISCLOSURE

No potential conflict of interest relevant to this article was reported.

REFERENCES

1. Loktev A, Lindner T, Mier W, et al. A tumor-imaging method targeting cancer-associated fibroblasts. *J Nucl Med.* 2018;59:1423–1429.
2. Balkwill FR, Capasso M, Hagemann T. The tumor microenvironment at a glance. *J Cell Sci.* 2012;125:5591–5596.
3. Lindner T, Loktev A, Altmann A, et al. Development of quinoline-based theranostic ligands for the targeting of fibroblast activation protein. *J Nucl Med.* 2018;59:1415–1422.
4. Kratochwil C, Flechsig P, Lindner T, et al. ^{68}Ga-FAPI PET/CT: tracer uptake in 28 different kinds of cancer. *J Nucl Med.* 2019;60:801–805.
5. Sollini M, Kirienko M, Gelardi F, Fiz F, Gozzi N, Chiti A. State-of-the-art of FAPI-PET imaging: a systematic review and meta-analysis. *Eur J Nucl Med Mol Imaging.* 2021;48:4396–4414.
6. Kuwert T, Schmidkonz C, Prante O, Schett G, Ramming A. FAPI-PET opens a new window for understanding of immune-mediated inflammatory diseases. *J Nucl Med.* 2022;63:1136–1137.
7. Schmidkonz C. Perspective on fibroblast activation protein–specific PET/CT in fibrotic interstitial lung diseases: imaging fibrosis—a new paradigm for molecular imaging? *J Nucl Med.* 2022;63:125–126.
8. Calais J. FAP: the next billion dollar nuclear theranostics target? *J Nucl Med.* 2020;61:163–165.
9. Ferdinandus J, Costa PF, Kessler L, et al. Initial clinical experience with ^{90}Y-FAPI-46 radioligand therapy for advanced-stage solid tumors: a case series of 9 patients. *J Nucl Med.* 2022;63:727–734.
10. Croft AP, Campos J, Jansen K, et al. Distinct fibroblast subsets drive inflammation and damage in arthritis. *Nature.* 2019;570:246–251.
11. Gurtner GC, Werner S, Barrandon Y, Longaker MT. Wound repair and regeneration. *Nature.* 2008;453:314–321.
12. Schmidkonz C, Rauber S, Atzinger A, et al. Disentangling inflammatory from fibrotic disease activity by fibroblast activation protein imaging. *Ann Rheum Dis.* 2020;79:1485–1491.
13. Stone JH, Zen Y, Deshpande V. IgG4-related disease. *N Engl J Med.* 2012;366:539–551.

14. Della-Torre E, Feeney E, Deshpande V, et al. B-cell depletion attenuates serological biomarkers of fibrosis and myofibroblast activation in IgG4-related disease. *Ann Rheum Dis.* 2015;74:2236–2243.
15. Zhang W, Stone J. Management of IgG4-related disease. *Lancet Rheumatol.* 2019;1:E55–E65.
16. Wohlfahrt T, Rauber S, Uebe S, et al. PU.1 controls fibroblast polarization and tissue fibrosis. *Nature.* 2019;566:344–349.
17. Luo Y, Pan Q, Yang H, Peng L, Zhang W, Li F. Fibroblast activation protein–targeted PET/CT with ^{68}Ga-FAPI for imaging IgG4-related disease: comparison to ^{18}F-FDG PET/CT. *J Nucl Med.* 2021;62:266–271.
18. Distler O, Assassi S, Cottin V, et al. Predictors of progression in systemic sclerosis patients with interstitial lung disease. *Eur Respir J.* 2020;55:1902026.
19. Tyndall AJ, Bannert B, Vonk M, et al. Causes and risk factors for death in systemic sclerosis: a study from the EULAR Scleroderma Trials and Research (EUSTAR) Database. *Ann Rheum Dis.* 2010;69:1809–1815.
20. Bergmann C, Distler JH, Treutlein C, et al. ^{68}Ga-FAPI-04 PET-CT for molecular assessment of fibroblast activation and risk evaluation in systemic sclerosis-associated interstitial lung disease: a single-centre, pilot study. *Lancet Rheumatol.* 2021; 3:e185–e194.
21. Röhrich M, Leitz D, Glatting FM, et al. Fibroblast activation protein–specific PET/CT imaging in fibrotic interstitial lung diseases and lung cancer: a translational exploratory study. *J Nucl Med.* 2022;63:127–133.
22. Bondue B, Castiaux A, Van Simaeys G, et al. Absence of early metabolic response assessed by ^{18}F-FDG PET/CT after initiation of antifibrotic drugs in IPF patients. *Respir Res.* 2019;20:10.
23. Travers JG, Kamal FA, Robbins J, Yutzey KE, Blaxall BC. Cardiac fibrosis: the fibroblast awakens. *Circ Res.* 2016;118:1021–1040.
24. Aghajanian H, Kimura T, Rurik JG, et al. Targeting cardiac fibrosis with engineered T cells. *Nature.* 2019;573:430–433.
25. Haslbauer JD, Lindner S, Valbuena-Lopez S, et al. CMR imaging biosignature of cardiac involvement due to cancer-related treatment by T1 and T2 mapping. *Int J Cardiol.* 2019;275:179–186.
26. Totzeck M, Schuler M, Stuschke M, Heusch G, Rassaf T. Cardio-oncology: strategies for management of cancer-therapy related cardiovascular disease. *Int J Cardiol.* 2019;280:163–175.
27. Siebermair J, Köhler M, Kupusovic J, et al. Cardiac fibroblast activation detected by Ga-68 FAPI PET imaging as a potential novel biomarker of cardiac injury/remodeling. *J Nucl Cardiol.* 2021;28:812–821.
28. Heckmann MB, Reinhardt F, Finke D, et al. Relationship between cardiac fibroblast activation protein activity by positron emission tomography and cardiovascular disease. *Circ Cardiovasc Imaging.* 2020;13:e010628.
29. Cavalera M, Wang J, Frangogiannis NG. Obesity, metabolic dysfunction, and cardiac fibrosis: pathophysiological pathways, molecular mechanisms, and therapeutic opportunities. *Transl Res.* 2014;164:323–335.
30. Müller OJ, Heckmann MB, Ding L, et al. Comprehensive plasma and tissue profiling reveals systemic metabolic alterations in cardiac hypertrophy and failure. *Cardiovasc Res.* 2019;115:1296–1305.
31. Prabhu SD, Frangogiannis NG. The biological basis for cardiac repair after myocardial infarction: from inflammation to fibrosis. *Circ Res.* 2016;119:91–112.
32. Lafuse WP, Wozniak DJ, Rajaram MV. Role of cardiac macrophages on cardiac inflammation, fibrosis and tissue repair. *Cells.* 2020;10:51.
33. Sutton MGSJ, Sharpe N. Left ventricular remodeling after myocardial infarction: pathophysiology and therapy. *Circulation.* 2000;101:2981–2988.
34. Ørn S, Manhenke C, Anand IS, et al. Effect of left ventricular scar size, location, and transmurality on left ventricular remodeling with healed myocardial infarction. *Am J Cardiol.* 2007;99:1109–1114.
35. Kessler L, Kupusovic J, Ferdinandus J, et al. Visualization of fibroblast activation after myocardial infarction using ^{68}Ga-FAPI PET. *Clin Nucl Med.* 2021;46: 807–813.
36. Diekmann J, Koenig T, Thackeray JT, et al. Cardiac fibroblast activation in patients early after acute myocardial infarction: integration with magnetic resonance tissue characterization and subsequent functional outcome. *J Nucl Med.* 2022;63: 1415–1423.
37. Xie B, Wang J, Xi X-Y, et al. Fibroblast activation protein imaging in reperfused ST-elevation myocardial infarction: comparison with cardiac magnetic resonance imaging. *Eur J Nucl Med Mol Imaging.* 2022;49:2786–2797.
38. Wu M, Ning J, Li J, et al. Feasibility of in vivo imaging of fibroblast activation protein in human arterial walls. *J Nucl Med.* 2022;63:948–951.
39. Kupusovic J, Kessler L, Nekolla SG, et al. Visualization of thermal damage using ^{68}Ga-FAPI-PET/CT after pulmonary vein isolation. *Eur J Nucl Med Mol Imaging.* 2022;49:1553–1559.
40. Chen B-X, Xing H-Q, Gong J-N, et al. Imaging of cardiac fibroblast activation in patients with chronic thromboembolic pulmonary hypertension. *Eur J Nucl Med Mol Imaging.* 2022;49:1211–1222.
41. Mauritz G-J, Kind T, Marcus JT, et al. Progressive changes in right ventricular geometric shortening and long-term survival in pulmonary arterial hypertension. *Chest.* 2012;141:935–943.
42. Forfia PR, Fisher MR, Mathai SC, et al. Tricuspid annular displacement predicts survival in pulmonary hypertension. *Am J Respir Crit Care Med.* 2006;174: 1034–1041.
43. Gu Y, Han K, Zhang Z, et al. ^{68}Ga-FAPI PET/CT for molecular assessment of fibroblast activation in right heart in pulmonary arterial hypertension: a single-center, pilot study. *J Nucl Cardiol.* March 23, 2022 [Epub ahead of print].
44. Qin C, Song Y, Liu X, et al. Increased uptake of ^{68}Ga-DOTA-FAPI-04 in bones and joints: metastases and beyond. *Eur J Nucl Med Mol Imaging.* 2022;49:709–720.
45. Zheng S, Lin R, Chen S, et al. Characterization of the benign lesions with increased ^{68}Ga-FAPI-04 uptake in PET/CT. *Ann Nucl Med.* 2021;35:1312–1320.
46. Ge L, Fu Z, Wei Y, et al. Preclinical evaluation and pilot clinical study of ^{18}F-AlF-NOTA-FAPI-04 for PET imaging of rheumatoid arthritis. *Eur J Nucl Med Mol Imaging.* 2022;49:4025–4036.
47. Conen P, Pennetta F, Dendl K, et al. ^{68}Ga-FAPI uptake correlates with the state of chronic kidney disease. *Eur J Nucl Med Mol Imaging.* 2022;49:3365–3372.
48. Zhou Y, Yang X, Liu H, et al. Value of Ga-FAPI-04 imaging in the diagnosis of renal fibrosis. *Eur J Nucl Med Mol Imaging.* 2021;48:3493–3501.